An Overview of Atom-Based SI-traceable Electric-Field Metrology

*Joshua A. Gordon, Christopher L. Holloway, Matthew Simons
*Contact: Josh.gordon@nist.gov

National Institute of Standards and Technology
Communications Technology Laboratory, Boulder CO 80305

Abstract: We present an overview of radio frequency (RF) electric-field measurements using Rydberg atoms. This technique exploits the rich resonance response of these atoms which can occur across a large frequency range from about 500 MHz-500 GHz. This measurement utilizes alkali atoms such as rubidium and cesium atoms confined in a glass vapor cell that are excited optically by two different lasers to high energy Rydberg states. Once in the Rydberg state the atoms exhibit a significant response to RF fields. The presence of the RF field alters the optical spectrum of the atoms, which can be interrogated to determine the RF field strength. One of the main goals of this work is an atomic standard measurement of RF fields that is intrinsically calibrated, directly linked to the SI and atomic structural constants.

Key Words: Electric Field; Rydberg Atoms; Radio Frequency; Electromagnetically Induced Transparency (EIT)

I. Introduction

Over the past several years many advances have been made in using atoms to directly measure radio-frequency (RF) electric-fields [1-5]. In particular, a new technique for converting an RF field amplitude into an optical frequency response in a gas of atoms has shown much promise. The goal is an atomic standard measurement of RF fields that is intrinsically calibrated and directly linked to the SI. In this approach a gas of room temperature alkali atoms such as Rubidium (Rb) and Cesium (Cs) contained in a glass vapor cell are optically excited to a high enough energy that the atoms become resonant to RF fields. Two laser are used to accomplish this. One laser is used to excite the lower energy levels of the atoms while the second increases the atom's energy to the point that the outer most electron orbit is larger enough that the atom behave much like a hydrogen atom. Such an atom is referred to as a Rydberg atom [6] and can act like a nano-sized antenna which as we show can respond to RF fields.

While in the Rydberg state, the atom exhibits a large response, i.e. a large dipole moment, to RF-fields over the frequency range of about 500 MHz-1 THz. To the lasers, the atomic gas acts like a non-linear optical medium that experiences changes in electrical susceptibility when interacting with an RF field. More specifically, where the atomic gas would preferentially transmit a single optical frequency, in the presence of the RF-field two optical frequencies are preferentially transmitted. It can be shown that the difference in the two optical frequencies is linearly proportional to the applied RF-field amplitude. We will discuss the theory behind this technique and show how this technique provides an atomic linked SI traceable RF-field measurement. Experimental data are presented for electric fields radiated by antenna sources which are compared to electromagnetic theory and finite element simulations.

II. Atom Based Electric Field Measurement

a) Rydberg Atom Preparation

For the remainder of this paper we will focus on measurements made using Rb atoms. Rydberg atoms are prepared using two different wavelength lasers. The probe laser is tuned to excite the D_2 transition ($5S_{1/2} - 5P_{3/2}$) around $\lambda_p \cong 780\ nm$ (red) and the coupling laser is tuned to $\lambda_c \cong 480\ nm$ (blue) in order

to excite the final Rydberg states. Tuning the coupling laser to different wavelengths allows for different Rydberg states to be accessed. Figure 1 shows the scenario for the specific excitation of the $5P_{3/2} - nD_{5/2}$ transition, where n is the principle quantum number and depends on the exact λ_c chosen. The Rydberg state leads to a strong RF response of the atoms which manifests as the $nD_{5/2} - (n+1)P_{3/2}$ transition. These two lasers are aligned to counter propagate collinearly and are focused at the center of the vapor cell to a nominal $1/e$ beam diameter of around $100\ \mu m$. Beam powers for the probe and coupling laser are nominally 100 nW and 30 mW respectively. A dichroic filter which reflects λ_c and transmits λ_p is used to overlap the two beams. The probe transmission through the vapor cell is measured with a silicon photodiode detector. To reject unwanted signal from room lights, etc., a $10\ nm$ wide band pass filter centered at $780\ nm$ is placed in front the detector. Heterodyne detection of the *probe* beam signal using a nominal amplitude modulation of 20 kHz-30 kHz on the *coupling* laser beam aids in improving signal to noise and was used in the data we present here. Figure 2 shows the optical layout for generating Rb Rydberg atoms while simultaneously measuring the transmission of the probe beam.

b) E-Field Determined from Atom Vapor Optical Susceptibility

In this approach we wish to relate the optical response of the atoms to an incident RF field. This can be achieved by deriving the optical susceptibility, χ for a volume filled with a gas of alkali atoms excited through four energy levels. As a full derivation of the susceptibility is outside the scope of this paper, we refer the reader to [7] and [8] for an in depth theoretical treatment of this atomic system. Here we present the final results important for RF electric-field metrology. The imaginary part of the refractive index can be determined using the fact that $\sqrt{(1+\chi)} = n + jk$, where n is the real part and k the imaginary part of the refractive index which governs the degree of absorption experienced by the probe beam as it traverses the vapor cell.

In the case where only the probe laser is present and tuned to the D_2 transition, much of the light will be absorbed by the atoms. However, it can be shown that when both the probe (tuned D_2 transition) and the coupling (tuned to excite a Rydberg transition) lasers are present, a transparency window occurs where absorption of the probe laser is significantly reduced. This phenomenon is call Electromagnetically Induced Transparency (EIT) [9] and is observed as a *peak* in the *absorption* spectrum of the probe laser. Furthermore, when the RF field is also present and on resonance with the Rydberg transition, the EIT peak splits into two peaks. These two peaks occur above and below the center frequency of the D_2 transition, $f_{D2} = 384.23 \ldots THz$. It can be shown that the frequency separation of these two peaks, Δf_{probe} measured in the probe absorption spectrum is proportional to the RF field strength by [10],[11],

$$\Delta f_{Probe} = \frac{\lambda_c}{\lambda_p} \frac{\wp_{RF} |E_{RF}|}{2\pi\hbar} \qquad (1)$$

where $\wp_{RF}$ is the atoms dipole moment for the RF transition (much like the dipole moment of an antenna), $\hbar$ is Plank's constant, and $|E_{RF}|$ is the magnitude of the RF field and λ_c and λ_p are the wavelengths of the coupling and probe lasers respectively. With this a measurement of the RF electric field magnitude has been reduced to an optical frequency measurement. The probe laser spectrum with and without an RF field is shown in Figure 3. The splitting is clearly observed when an RF field at a frequency of 104.77 GHz is incident on the vapor cell. For reference this splitting corresponds to a strength of 2.8 V/m.

c) Broad RF Tunability

For each Rydberg state there is a corresponding RF transition and associated dipole moment. Therefore by changing the coupling laser wavelength, λ_c one can tune which RF frequency the atom responds to. This is shown in Figure 4 for two cases where the coupling laser is set to $\lambda_c = 479.32\ nm$ and $\lambda_c = 483.60\ nm$ in order to tune the atom's RF resonance from 2.03 GHz to 150.40 GHz. The RF transition frequency for a given coupling λ_c can be calculated using the total ionization energy of the atom and corresponding quantum

defects [11]. Results of such a calculation for all $nD_{5/2} - (n+1)P_{3/2}$ RF transitions from $20 \leq n \leq 130$ are shown in Figure 5. From this we see that the coupling laser need only change a few nanometers in order to tune the atom from about 500 GHz up to about 500 GHz. This shows the broad tunability of this technique throughout the radio, microwave, millimeter-wave, and sub-terahertz regimes.

d) Self-Calibration and SI-Traceability

From Equation (1) we see that Δf_{probe} is proportional to $|E_{RF}|$ and the atom's dipole moment, $\wp_{RF}$. The dipole moment is an intrinsic parameter of the atom and is also a constant for any given RF transition. It can be accurately determined using atomic spectra measurements and quantum theory [6]. All other variables, λ_c, λ_p , and $\hbar$ can be determined independent of the RF field and the dipole moment. This suggests this approach can lead to a self-calibrated electric field measurement because all free parameters can be known a priori to measuring the RF field.

Furthermore, through Equation (1) we see that $|E_{RF}|$ is proportional to Plank's constant. Therefore, the calculation of the RF-field strength based on the optical frequency measurement is linked to an SI constant. This also suggests a directly SI-traceable measurement. Progress is currently being made toward establishing a full traceability path where the uncertainties associated with each part of the measurement are well understood.

III. Measurements

We present measurement results for several RF frequencies. A block diagram of the setup that was used for these measurements is shown in Figure 6 which includes the vapor cell, source antenna, lock-in amplifier for heterodyne detection, photo diode detector, probe laser, and coupling laser. Measurements performed at 15.59 GHz, 17.04 GHz, and 104.77 GHz are shown in Figure 7 where the spitting is plotted versus the square root of the power input to the source antenna by the signal generator, $\sqrt{P_{SG}}$. The linear slope for the frequency splitting as predicted by Equation (1) is clearly observed as it should be since $\sqrt{P_{SG}} \propto |E_{RF}|$. These data were also compare to both analytical far-field calculations and full 3D finite element numerical simulations. These comparisons are shown in Figure 8. We see good agreement between the theoretically predicted values for the E-field strength and the values based on this Rydberg atom measurement. These data also demonstrate the large tunability of this measurement. We would like to point out that only one optical setup (Figure 6.) was needed to make these measurements across the ≈ 90 GHz frequency range, whereas three separate RF sources were required to generate the signals.

IV. Conclusion

In conclusion, we have given a short overview of a recently developed atom based technique for measuring RF fields over the frequency range of ≅ 500 MHz-500 GHz. This technique uses alkali atoms confined in a glass vapor cell that are excited to Rydberg states by two different lasers. An RF measurement is made by observing a frequency splitting in the optical spectrum of the atomic gas when an RF field is present. This frequency splitting is proportional to the magnitude of the applied RF field. We present a brief theoretical description of how the applied RF field can be interpreted from an all-optical measurement and provide reference for further in depth reading. We present data of E-field measurements at 15.59 GHz, 17.04 GHz, and 104.77 GHz using this technique which are compared to both analytical far-field and 3D finite element simulations. These data show the broadly tunable capability of this technique and the theoretical predicted linearity of the optical spectral to applied RF fields. This technique shows much promise for realizing a self-calibrating, SI-traceable, and broadly tunable E-field measurement that is linked to atomic constants.

V. References

[1] J. A. Gordon, C. L. Holloway, A. Schwarzkopf, D. A. Anderson, S. A. Miller, N. Thaicharoen, and G. Raithel,Appl. Phys. Lett. 105, 024104 (2014)

[2] C. L. Holloway, J. A. Gordon, S. Jefferts, A. Schwarzkopf, D. A. Anderson, S. A. Miller, N. Thaicharoen, and G. Raithel, IEEE Trans. Antennas Propag. Soc. (2014).

[3] C. L. Holloway, J. A. Gordon, A. Schwarzkopf, D. A. Anderson, S. A. Miller, N. Thaicharoen, and G. Raithel, Appl. Phys. Lett. 104, 244102 (2014).

[4] J. A. Sedlacek, A. Schwettmann, H. Kubler, R. Low, T. Pfau, and J. P. Shaffer, Nature Phys. 8, 819 (2012).

[5]J. A. Sedlacek, A. Schwettmann, H. Kubler, and J. P. Shaffer, Phys. Rev. Lett. 111, 063001 (2013).

[6] T. F. Gallagher, Rydberg Atoms (Cambridge University Press, 1994).

[7] S. N. Sandhya and K. K. Sharma, Phys. Rev. A 55, 2155 (1997).

[8] P. Meystre and M. Sargent III, Elements of Quantum Optics, 4th Ed. Springer, chapter 9, 2007.

[9] K. J. Boller, A. Imamoglu, and S. E. Harris, Phys. Rev. Lett. 66, 2593 (1991).

[10] S. H. Autler and C. H. Townes, Phys. Rev. 100, 703 (1955).

[11] T. Y. Abi-Salloum, Phys. Rev. A 81, 053836 (2010).

VI. Acknowledgments

This work was funded in part by the DARPA QuASAR program.

VII. Figures

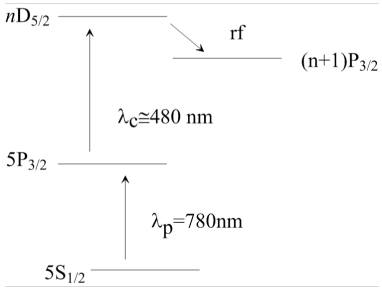

Figure 1. Rb energy levels for generating Rydberg states for $n \gtrsim 20$. Atomic transitions for the different photon energies of the probe, coupling and RF fields are shown.

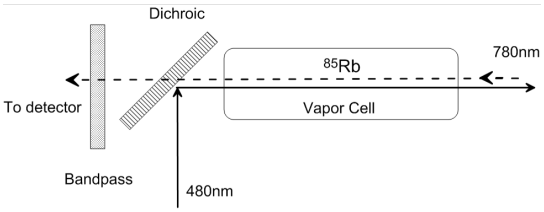

Figure 2. Optical layout for generating Rydberg atoms in a vapor cell full of ^{85}Rb atoms and detecting probe laser transmission. (Dotted) The probe and (Solid) coupling laser are in actuality overlapping for these measurements, but are shown here displaced for clarity.

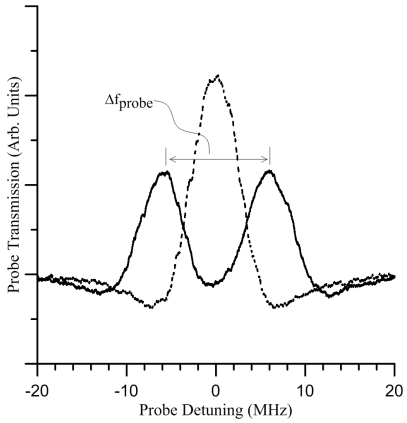

Figure 3. Optical spectrum for the probe laser with (solid) an RF field of 2.8 V/m at 104.77 GHz is incident on the vapor cell and without (dotted) the RF field present. The splitting of the EIT peak resulting from the RF field is clearly visible.

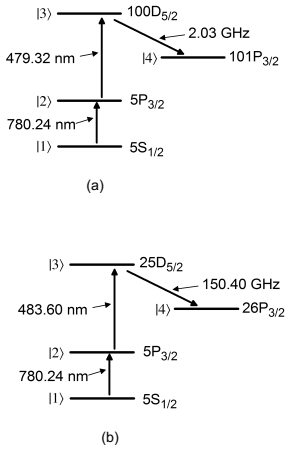

Figure 4. Tuning of the RF transition by changing the coupling laser wavelength, λ_c. (a) For $\lambda_c = 479.32\ nm$, the atoms will respond to an RF frequency 2.03 GHz. (b) For $\lambda_c = 483.60\ nm$, the atoms will respond to an RF frequency 150.40 GHz.

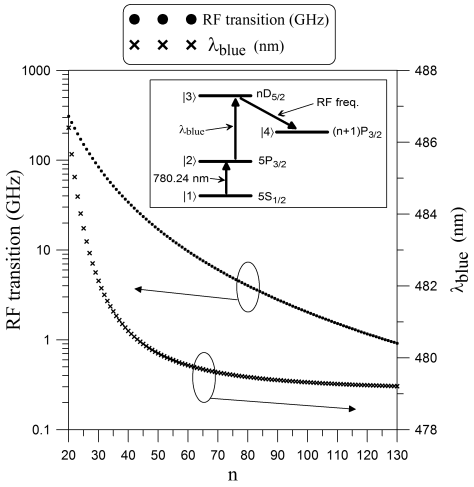

Figure 5. RF tuning range of the atoms for changing coupling (blue) laser wavelength for the $nD_{5/2} - (n+1)P_{3/2}$ transitions.

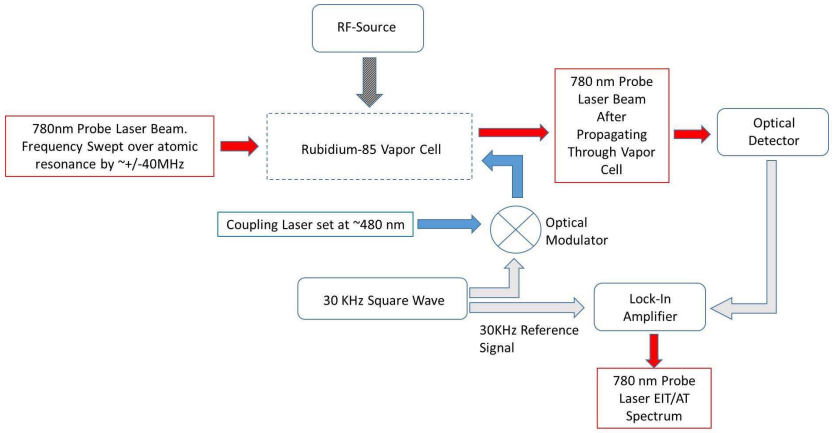

Figure 6. Experimental layout block diagram.

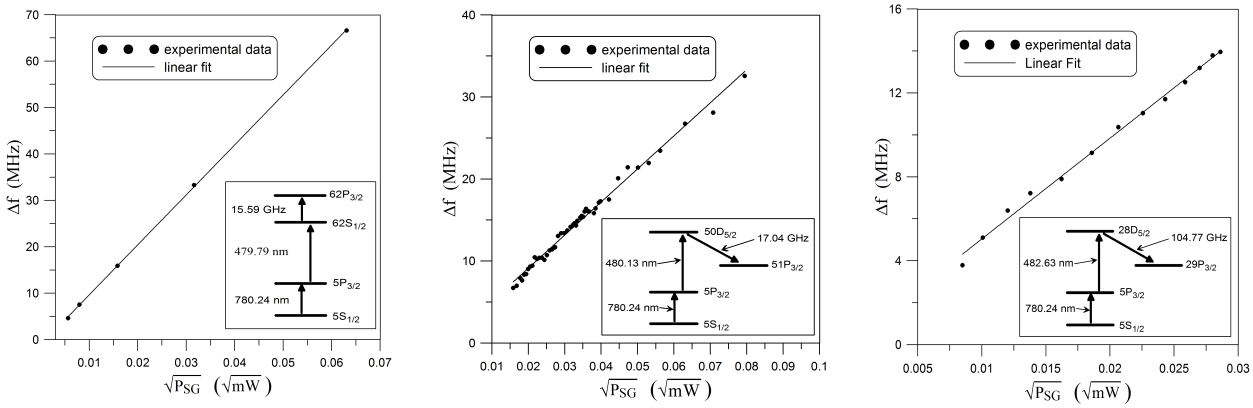

Figure 7. Linearity of the frequency splitting on the probe laser spectrum versus $\sqrt{P_{SG}}$ (the square root of the input power to the source antenna from the signal generator). Measurements for RF frequencies of 15.59 GHz, 17.04 GHz, and 104.77 GHz respectively are shown. Linear least squares fits are also shown.

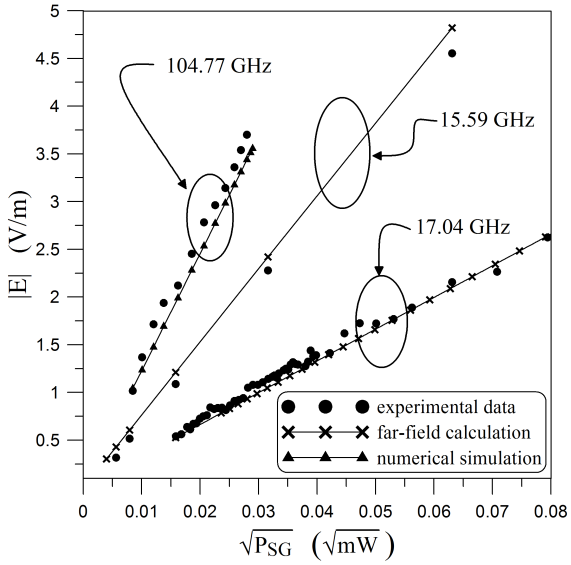

Figure 8. E-field as determined from the frequency splitting of Figure 7. Data are compared to analytical far-field calculations and 3D finite element simulations.